DOI 10.14622/Advances_49_2023_13

Ink spreading in gravure printing

Armin Weichmann, Thomas Sprinzing and Matthias Galus

Hochschule der Medien Stuttgart, Institut für Angewandte Forschung (IAF), Nobelstr. 10, 70569 Stuttgart, Germany
E-mails: weichmann@hdm-stuttgart.de; sprinzing@hdm-stuttgart.de; galus@hdm-stuttgart.de

Short abstract

Even though gravure printing is a process that has been known for a long time, it is rare to find a consistent model in the literature of what happens during the doctoring of the ink and the ink transfer. This article deals with the aspect of ink spreading on substrates and its influencing factors. A model on the basis of the Murray-Davies formula and Lambert-Beer's law is presented that can explain essential effects of the ink spreading in gravure. Within a large-scale gravure printing trial on an industrial-scale web press a subset of the varied parameters were chosen to expose the influencing factors: printing velocity (120, 180, 240 m/min), ink viscosity (high, medium, low), electrostatic assist (ESA) (on, off) on film with organic solvent based ink. The effect of ink spreading is measured by spot colour tonal value (SCTV). The results show that the factors behave completely differently in the tonal range of single dots, where spreading plays a role as opposed to the tonal range with a closed ink layer. With single dots viscosity plays the major role as it influences ink spreading most.

Keywords: rotogravure, ink spreading, parameter study, quality control

1. Introduction and background

Commercial rotogravure is actually a long-established process. On the other hand, fluid transfer in gravure printing is a complex process. In the last decades, researchers like Kunz (1975), Hübner (1991), Kumar (2015), Grau, et al. (2016) and Schäfer, et al. (2019) have contributed to a deeper understanding. More recently, Brumm, et al. (2021a; 2021b) tried to classify transfer patterns on the basis of a neural network.

Nevertheless, the scientific literature rarely provides an overall view of how individual steps in the process influence the print result. A comprehensive view is offered in trade journals, e.g. as a guide to troubleshooting in gravure printing (Beilenhoff, 2011a; 2011b). Joshi (2016) conducted an extensive Design of Experiments aimed at the optimising of mottle and missing dots. This article uses a similar approach to proof the different factors and their strength of influence on the gradation of a gravure print with an especial distinction between the area of single dots and the area after the flooding, where a closed layer of ink is printed.

This is a result in the frame of a large-scale gravure printing trial, that was conducted to systematically investigate the influence of seven major printing parameters (printing velocity, type of ink, ink viscosity, type of substrate, electrostatic assist (ESA) and doctor blade angle) on hydrodynamic pattern formation and gravure print quality. The trial itself is described in detail in Brumm, et al. (2022).

2. Model and assumptions to ink spreading

2.1 Effect of ink spreading on the tonal value of a print

A dot in a regular grid is assigned a space that corresponds to the size of a unit cell of the grid and is bounded by the neighbouring cells. Let the area reserved for each dot be A (see Figure 1). Two dots are considered that have the same ink volume and the same ink composition, i.e. the same amount of pigment. One of the two spreads more than the other. Let the proportion of covered area for the less spreading dot D be φ = area$(D)/A$, its layer thickness $h/2$, φ' = area$(D')/A$ be the proportion of covered area for the more spreading, i.e. larger, but flatter dot D', $h'/2$ its thickness. ($0 < \varphi, \varphi' < 1$)

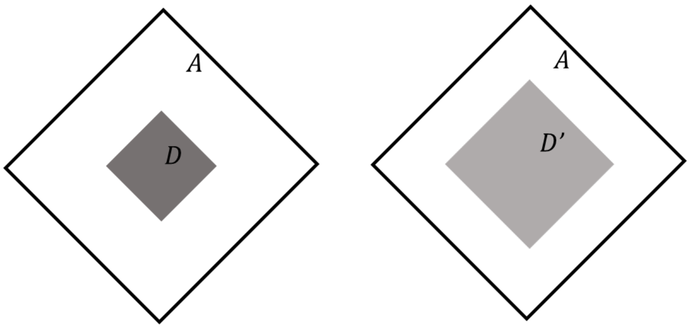

Figure 1: (a) Gravure dot D within its elementary cell of area A; (b) the more spreading dot D' within its elementary cell of area A

In a simplified model, the printed ink layer is regarded as a colour filter with a first passage of light, then the reflection by the surface and a second passage of light. In this approximation the surface is assumed to be perfectly reflective. As the light passes the layer twice the overall layer thickness can be assumed to be $h/2 + h/2 = h$. Additionally, the ink layer of the dot is considered to have the same thickness everywhere. If the dot spreads more, then it becomes larger. Nevertheless, it is considered to have a reduced but still homogeneous thickness.

Since the volume V_{dot} of the transferred ink remains the same, the following applies:

$$A\,\varphi\,h = A\,\varphi'\,h' = V_{\text{dot}} \qquad [1]$$

With Equation [2] $\Delta a = \dfrac{\varphi' - \varphi}{\varphi}$ one can express the area coverage φ' as

$$\varphi' = \Delta a\,\varphi + \varphi = \varphi(1 + \Delta a) \qquad [3]$$

where Δa represents the relative increase in area due to the increased spreading. Δa = 10 % means, for example, an increase in area of 10 %. With Equation [3] the layer thickness of the more spreading point is then calculated from Equation [1] as:

$$h' = h\frac{\varphi}{\varphi'} = \frac{h}{1 + \Delta a} \qquad [4]$$

The absorption of light occurs through the pigments in the ink and can be described by Lambert-Beer's law.

$$I_{\mathrm{F}} = I_0\,e^{-\tau h} \qquad [5]$$

with I_{F} : light intensity after passing the ink layer, I_0 : incident light intensity, τ : absorption coefficient, and h : ink layer thickness.

Thus the intensity for the dot together with its reserved area:

$$I_{\mathrm{P}} = (1 - \varphi)\,I_0 + \varphi\,I_{\mathrm{F}} = (1 - \varphi)I_0 + \varphi e^{-\tau h} I_0 = (1 - \varphi + \varphi e^{-\tau h})\,I_0 \qquad [6]$$

The first part is essentially the Murray-Davis formula in intensity notation. $(1 - \varphi)\, I_0$ describes the light intensity generated by the uncovered surface that has no absorption. $\varphi\, I_F = \varphi\, I_0\, e^{-\tau h}$ describes the light intensity that is added by the residual intensity after absorption by the dot. The ratio of the light intensities from the two dots is given by:

$$R_A = \frac{I_D'}{I_D} = \frac{I_0\left(1 - \varphi' + \varphi' e^{-\tau h'}\right)}{I_0(1 - \varphi + \varphi e^{-\tau h})} = \frac{1 - \varphi(1 + \Delta a) + \varphi(1 + \Delta a)e^{-\frac{\tau h}{(1+\Delta a)}}}{1 - \varphi + \varphi e^{-\tau h}} \quad [7]$$

Further

$$R_A = \frac{1 - \varphi(1 + \Delta a) + \varphi(1 + \Delta a)e^{-\frac{\tau h}{(1+\Delta a)}}}{1 - \varphi(1 + \Delta a) + \varphi\Delta a + \varphi e^{-\tau h}} = \frac{\varphi_T + \varphi(1 + \Delta a)e^{-\frac{\tau h}{(1+\Delta a)}}}{\varphi_T + \varphi(\Delta a + e^{-\tau h})} \quad [8]$$

where $\varphi_T = 1 - \varphi\,(1 + \Delta a)$ describes the area within *A* that remains uncovered at the more spreading dot *D'* (see Figure 1) and thus has no absorption. This term is the same for both dots. It is therefore sufficient to look at the remaining term to prove that the more spreading dot *D'* has a lower residual intensity and thus a higher colour intensity. Without φ_T and by reducing the factor φ the quotient R_D results from Equation [8] in

$$R_D = \frac{(1 + \Delta a)\, e^{-\frac{\tau h}{(1+\Delta a)}}}{\Delta a + e^{-\tau h}} \quad [9]$$

This quotient describes the brightness ratio of the two dots alone, i.e. it refers to the area occupied by the more spreading dot *D'*. The completely ink covered area of the larger point *D'* is compared with the combination of the thicker but smaller dot *D* and the additional uncovered area, which together give the area of dot *D'*.

As an example a typical absorption for the ink layer of density 1.0 is assumed. This density results from an absorption of 90 % of the light, while 10 % remains. Thus acc. to Equation [5]

$$\frac{I_F}{I_0} = 0.1 = e^{-\tau h} \text{ and } \tau d = 2.3 \quad [10]$$

This is conservative, at least for process colours, which usually have a reasonably higher density. If we now evaluate the Equation [9] for this density, we get

$$R_D = \frac{(1 + \Delta a)\, e^{-\frac{2.3}{(1+\Delta a)}}}{\Delta a + e^{-2.3}} \quad [11]$$

For Δa = 0 ... 40 % the following Table 1 is calculated for R_A and R_D. For the calculation of R_A, a medium-sized (first) dot *D* with an area coverage φ = 40 % is assumed.

It can be clearly seen that $R_D < 1$ for $\Delta a > 0$, i.e. the numerator of R_D is also always smaller than the denominator. Thus the residual intensity of the more spreading dot is smaller than that of the less spreading dot. For R_D this is a massive effect with 6 % decrease in intensity with only 1 % more spreading. For the entire grid cell, the decrease in intensity is smaller, but the effect is still significant.

Table 1: Brightness ratio R_D of the two dots D and D' and brightness ratio R_A of the two dots D and D' together with uncovered area of their grid space A against the relative spreading Δa of D'

Δa	R_D	$R_A(\varphi = 40\ \%)$
0 %	100 %	100.0 %
1 %	94 %	99.6 %
2 %	89 %	99.2 %
3 %	85 %	98.8 %
4 %	81 %	98.4 %
5 %	78 %	98.0 %
10 %	68 %	96.0 %
15 %	62 %	94.1 %
20 %	59 %	92.3 %
25 %	57 %	90.5 %
30 %	55 %	88.8 %
35 %	55 %	87.2 %
40 %	54 %	85.7 %

2.1 Influences of process parameters on ink spreading

Various factors of printing influence the spreading of the ink on the substrate. A well-founded assumption is, that dot spreading is enhanced by lowering the ink viscosity, as this promotes the "mobility" of the ink and the increased solvent content means that the ink remains liquid for longer when drying and thus has more time to spread.

Further our assumption is that spreading of the dots is enhanced by the application of ESA, which promotes the emptying of the cells and draws the ink onto the substrate. Therefore, the electrostatic force supports the capillary forces, the emptying of the cells is more complete and more ink is transferred.

Slower printing speed is assumed to reduce the ink loss doctored out of the cells. As a result, more ink remains in the cells and more ink is transferred, leading to a higher colour intensity. This effect should be effective across the entire gradation, i.e. both in the area of visible dots and after flooding in the area of the fully covered ink layer. However, since more ink leads both to a directly higher ink thickness and to more spreading, the effect is stronger in the dot area. On the other hand, the slower printing speed leads to increased drying of the ink in the cells before transfer, which in turn can lead to less ink transfer or reduced spreading due to the higher viscosity.

From these assumptions it can be deduced that in the area of dot transfer, i.e. before flooding, a reduced viscosity and the use of ESA should play the most significant roles. Both factors, on the other hand, should no longer or considerably less be visible in the area of the fully covered ink layer.

3. Materials and methods

3.1 Gravure printing trial

3.1.1 Printing form layout

We used an electromechanically engraved, chrome-plated printing form (circumference 700 mm, engraving width 590 mm). The printing form was engraved on a Hell K500 engraving system (Hell Gravure Systems GmbH & Co. KG, Kiel, Germany) with a stylus angle 120°. The relevant raster angle for this article is Hell engraving angle 0 with raster frequency 80 lines/cm displayed in cyan. Angle 0 realises a compressed cell shape with a raster angle of 36.87° and an effective raster frequency of 80 lines/cm. The wedge with 28 tonal values (0, 1, 2, 3, 4, 5, 8, 10, 15, 20, 25, 30, 35, 40, 45, 50, 55, 60, 65, 70, 75, 80, 85, 90, 93, 95, 98, 100 %) in the lower part of area (C) is the relevant part in the print form layout for this article, see Figure 2. The print form layout was developed for use with the analysing methods as described in Brumm, et al. (2022).

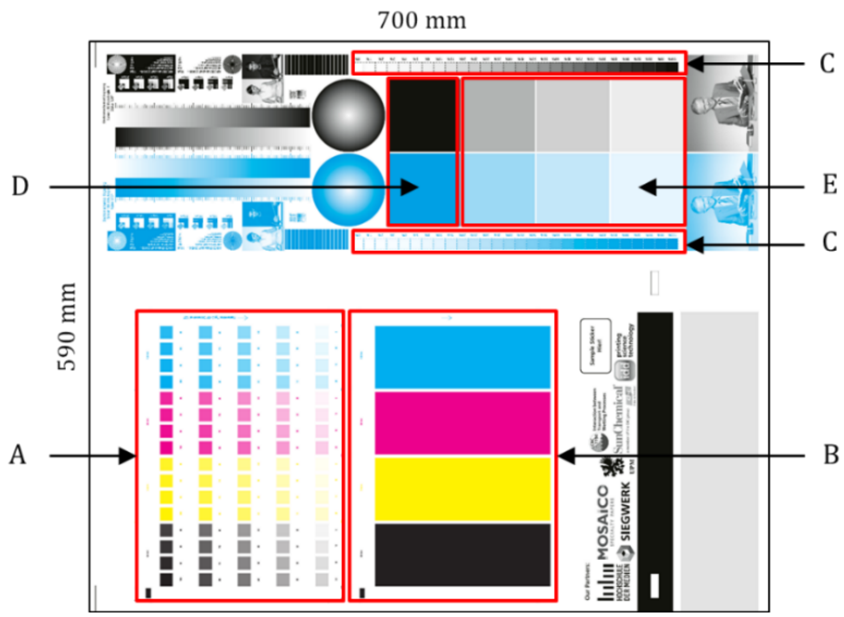

Figure 2: Print form layout; lower part of C is used for gradation measurements

3.1.2 Design of experiments

A 3-day printing trial was conducted on an industrial-scale gravure printing machine Bobst Rotomec MW 60 (Bobst, Mex, Switzerland) with a printing form cylinder of 700 mm circumference and 700 mm face and a maximum printing speed of 300 m/min. The design of experiments uses seven factors, which are varied during the trial. The trial itself is described in detail in Brumm, et al. (2022). The design of experiments was based on ascending velocity ramps with the printing velocities 15, 30, 60, 90, 120, 180 and 240 m/min as target velocities. ESA was always turned off for 15 m/min and 30 m/min and was turned both off and on for the other printing velocities. Furthermore, the ink viscosity and the angle of the doctor blade were varied in three steps (high, medium, low). The water-based ink was prepared using four different viscosities (base, high, medium, low). For diluting the solvent-based inks, a nearly azeotropic mixture of ethanol (30 %) and ethyl acetate (70 %) was used. The water-based ink was diluted with tab water. The ambient temperature and humidity were recorded and the ink temperature was monitored during the printing trial. Printing ink viscosity was measured with a 4 mm ISO flow cup and was controlled with a Fasnacht Viscopoint IL CPS viscosity sensor in combination with a viscosity control system Fasnacht pentasmart. Doctor blade pressure (1.5 bar), impression roller pressure (1.5 bar) as well as impression roller hardness (80 Shore A) were kept constant. In total, 17 velocity ramps were performed with 12 parameter combinations each. For each parameter combination, 20 sheets (each 600 mm × 700 mm) were manually cut out, which results in over 4 000 sheets in total. The sheets were post-processed and evaluated according to the chosen analyzing method which mostly required further cutting as well as digitization steps. The areas A and B were used for classification of patterns with deep learning and Fourier analysis of ribbing patterns. The areas C were used for gradation measurements. With areas D and E mottle values and missing dots were evaluated.

For this article, only a small section of the large DoE is used, which is described below, considering factors:

- Printing velocity: Three different velocities from the trial, 120, 180 and 240 m/min, were used for this DoE.
- ESA: Two settings were used: off and on with 1 mA current (Enulec, Trittau, Germany, ESA1000compact), which is nearly maximum.
- Ink viscosity: Three different viscosities were used with the solvent based inks: high = 24 sec ISO#4, medium = 20 sec ISO#4, low = 17 sec ISO#4 (DIN EN ISO 2431) (Deutsches Institut für Normung, 2019).

Solvent based ink optimised for film (NC 133-15, magenta, Siegwerk, Siegburg, Germany) was printed on film (WSS 20 BoPP solid white film, both sides heat sealable, treated, Taghleef Industries, Dubai, United Arab Emirates). The patches with Hell gravure angle 0 (cyan colour in Figure 2) were measured for the evaluation. The ambient temperature and humidity were recorded and the ink temperature was monitored during the printing trial.

3.2 Sample analysis – gradation measurements

A measure of colour intensity is the Spot Colour Tonal Value (SCTV) according to ISO 20654:2017 (International Organization for Standardization, 2017), which is calculated from the CIE $L^*a^*b^*$ values in relation to the 100 % solid tone and normalised to paper white. The higher the SCTV, the stronger the colour of the measured field. For investigating the ink spreading this number, like dot gain, is especially advantageous, as both calculations reference to the solid tone. This leaves the relative colour intensity of the different tonal values in respect to the solid.

The gradation measurements were performed on the tonal value wedge over the whole tonal range (28 steps, see Section 3.1.2) of part C (Figure 2). The spectral values were measured by a Techkon SpectroDens spectro-densitometer (TECHKON GmbH, Königstein im Taunus, Germany) and stored as a spectrum and as CIE $L^*a^*b^*$ values.

Three substrate sheets were evaluated for each test point. Each colour wedge was measured three times so that measurement errors could be identified and corrected immediately. The resulting nine CIE $L^*a^*b^*$ measurements per colour field were averaged. From these SCTV were calculated and subtracted from the nominal tone values. The resulting curve, called dSCTV, should ideally be a horizontal line with the value 0.

4. Results and discussion

4.1 Tonal area evaluation

The factors speed, ESA and viscosity (see 3.1.1) result in 18 different factor combinations. As an example of the effect of the factors on spreading a section of the 50 % tonal values patches of EFMvhamV180E0, EFMvmamV180E0 and EFMvlamV180E0 (= all three samples at 180 m/min and ESA off, with high, medium and low viscosity) are shown in Figure 3. The increase in dot area is clearly visible, as is the reduction in intensity.

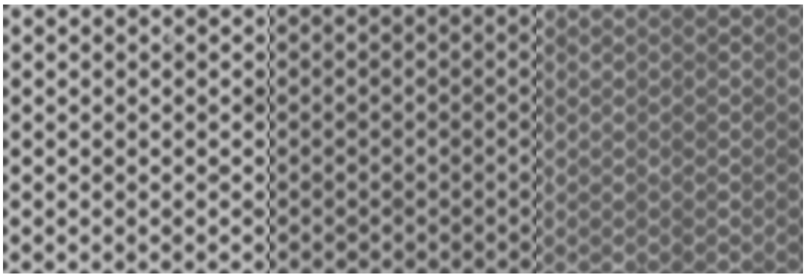

Figure 3: 50 % tonal values patches of EFMvhamV180E0, EFMvmamV180E0 and EFMvlamV180E0 (organic solvent based ink on film with 180 m/min and ESA off, high viscosity left, medium viscosity middle, low viscosity right picture) Hell gravure angle 0, 80 lines/cm, scanned with 1 200 dpi

The dSCTV curves of this configuration are shown in Figure 4.

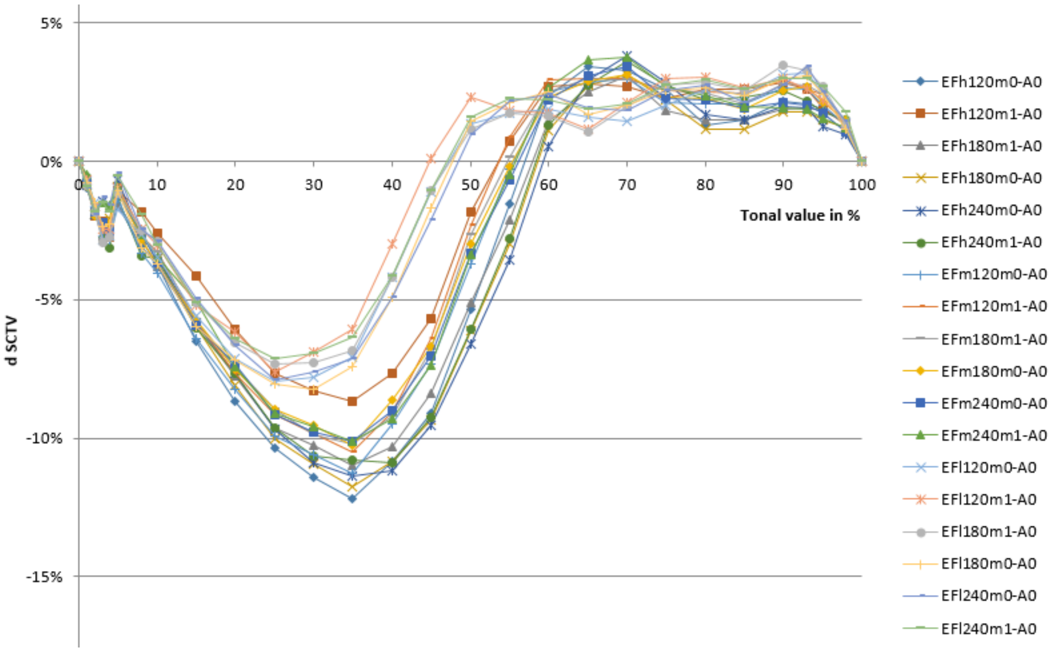

Figure 4: The dSCTV (= SCTV – TV) curves for different test points (legend for EFvsssme-A0: E – ethyl-based ink, F – film, v – viscosity (l, m, h), sss – speed (120, 180, 240), m – middle blade angle, e – ESA (0/1))

The dSCTV values in the area of the single dots (low tonal values up to ca. 60 %) are significantly negative, as the gradation used was not optimally adapted for these printing conditions. Nevertheless, there are clear differences for the different printing conditions. To further elaborate these differences, the centre point of the DoE was taken as reference (EFm180m1: viscosity = m, speed = 180 m/min, ESA = 1) and all values were related to this reference. Then the curves in Figure 5 result.

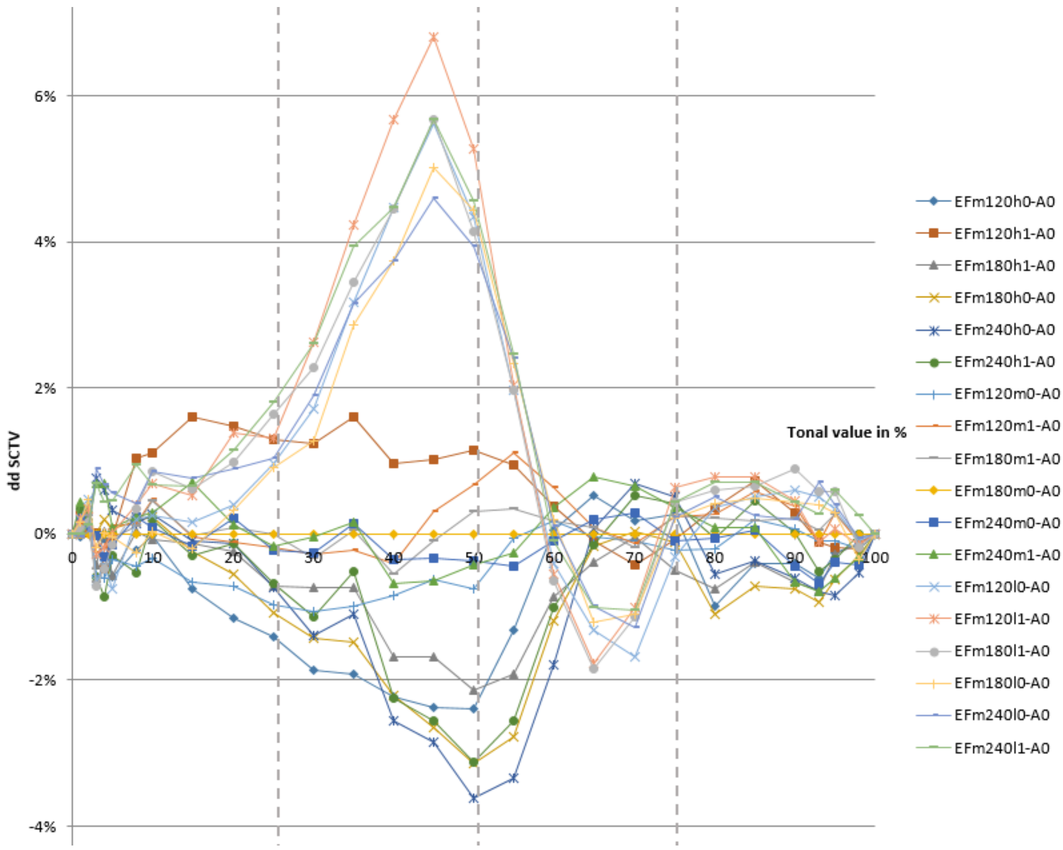

Figure 5: The ddSCTV (= SCTV – TV referenced to EFm180m1) curves for different test points; the dashed lines indicate the 3 tonal values used in the ANOVA evaluation (legend fo EFvsssme-A0: E – ethyl-based ink, F – film, v – viscosity (l, m, h), sss – speed (120, 180, 240), m – middle blade angle, e – ESA (0/1))

The four curves with the highest values in the 50 % range belong to the low viscosity, the four with the lowest values to the high viscosity. This already shows that viscosity plays the most important role and it works in different directions for the dots and the homogeneous areas.

To further illustrate these facts, the colour deviation in dE (DE2000) and the chromaticity differences dC (ΔC^*_{ab}) of the 50 % tonal value fields as well as the 75 % tonal values in relation to the trial point Efm180m0 (medium viscosity, medium speed – 180 m/min, ESA off) are plotted in Table 2 for tonal value 50 % and in Table 3 for tonal value 75 %. In contrast to 50 % tonal value, which is within the dot area, the 75 % tonal value is in the range where in rotogravure a more or less homogeneous ink film covers the complete grid cell.

Table 2: Left: dE values and right: dC values of patches in relation to patch with medium viscosity, medium speed – 180 m/min, ESA off for the 50 % tonal value; the value of EFm120h1 for 50 % was measured an outlier and is omitted for clarity

dE	ESA	off			on		
50%	Visco.	h	m	l	h	m	l
Speed	120	1,58	0,23	2,75		0,76	3,09
	180	2,26	**0,00**	2,72	1,21	0,41	2,67
	240	2,80	0,38	2,33	2,21	0,52	2,67

dC	ESA	off			on		
50%	Visco.	h	m	l	h	m	l
Speed	120	-3,99	-0,63	4,70		1,27	5,45
	180	-4,96	**0,00**	4,49	-2,89	0,43	4,35
	240	-6,49	-0,94	3,45	-4,94	-1,55	4,05

Table 3: Left: dE values and right: dC values of patches in relation to patch with medium viscosity, medium speed – 180 m/min, ESA off for the 75 % tonal value

dE	ESA	off			on		
75%	Visco.	h	m	l	h	m	l
Speed	120	1,14	0,24	2,20	1,14	0,37	1,85
	180	0,63	**0,00**	1,98	0,54	0,25	2,07
	240	0,70	0,26	2,39	0,49	0,29	2,35

dC	ESA	off			on		
75%	Visco.	h	m	l	h	m	l
Speed	120	0,68	0,04	-1,78	0,92	0,05	-1,69
	180	0,55	**0,00**	-1,83	0,50	-0,09	-1,93
	240	0,45	-0,12	-1,89	0,41	-0,12	-1,90

As can be seen the dE values are overall smaller with 75 % and the viscosity change makes the biggest difference in both tonal values. However, dE is not sensitive to directions. So dC is more interesting. For dots the chroma increases very significantly towards lower viscosity with dC at least +7 and up to +10 between high and low. This matches with the described model. For the homogeneous area the chroma does not increase, but in the contrary decreases in the range of dC = −2.5. This is due to the lower pigment content and the lack of the possibility for spreading. In the dot area, the actual difference in chroma due to spreading should therefore be even greater, as the pigment concentration also decreases there with lower viscosity. From the values for the 75 % tonal value, this additional chroma difference should be also more than 2.

4.2 Evaluation by ANOVA multivariance analysis

These results can be quantified by a multivariance analysis. This was done with a Java program written by Weichmann (2015) according to Montgomery (2021) and Backhaus, et al. (2018). The programme is specifically designed to handle multiple factor subsets of a Design of Experiments with a variety of effects to be used in the evaluation of the whole trial. The effects used here are in accordance to 4.1 the SCTV value of the 50 % tonal value field and the 75 % tonal value field and additionally the 25 % tonal value field for a second value in the dot area.

The Pareto diagram of the effects and the main effects plot are used to graphically display the significance of the different factors. In the Pareto diagram the factors are standardized to the critical value of the F-distribution for an error probability of 5 %. The x-axis shows the ratio of the factors' effect and the critical f-value for the degrees of freedom for this effect for an error probability of 5 %. So the value 1 (green dashed line in Figures 4 and 5) represents the critical value for the effect. Values above 1 are significant and values below are not significant in respect to the 5 % error probability. The higher the value, the more significant the factor for this effect. A value of 2.5 e.g. means that this factor exceeds this critical value by a factor of 2.5 and is therefore clearly significant. On the y-axis the factors and the interactions of two factors are listed.

The diagram of the effects' mean values for each level of each main factor shows the reaction of the effect to the variation of the factor. The y-axis plots the dSCTV value, the x-axis marks the different settings of the factor.

The following diagrams (Figures 6, 7 and 8) show the results of the dSCTV values for the three tonal values 25 %, 50 % and 75 %.

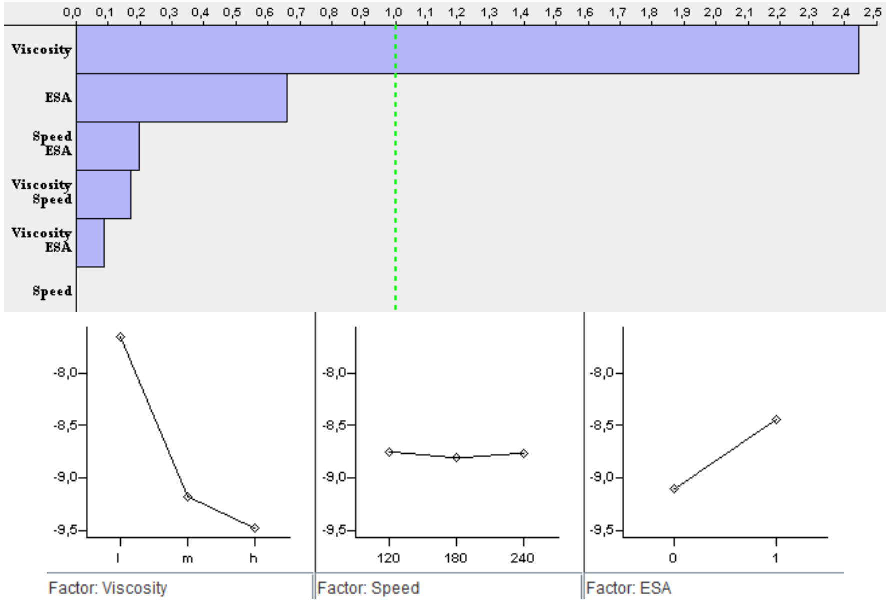

Figure 6: ANOVA evaluation of SCTV for TV = 25 %
Pareto diagram (x-axis: ratio between critical value of f-distribution and factor's value) and mean values of the test points with respective factor level (y-axis: dSCTV value, negative for 25 % tonal value)

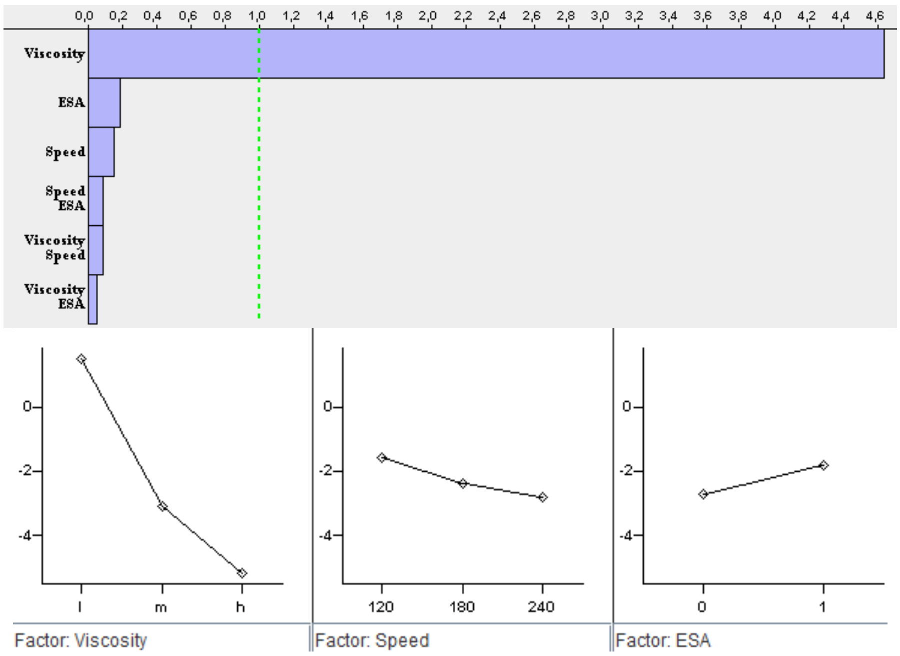

Figure 7: ANOVA evaluation of SCTV for TV = 50 %
Pareto diagram (x-axis: ratio between critical value of f-distribution and factor's value) and mean values of the test points with respective factor level (y-axis: dSCTV value)

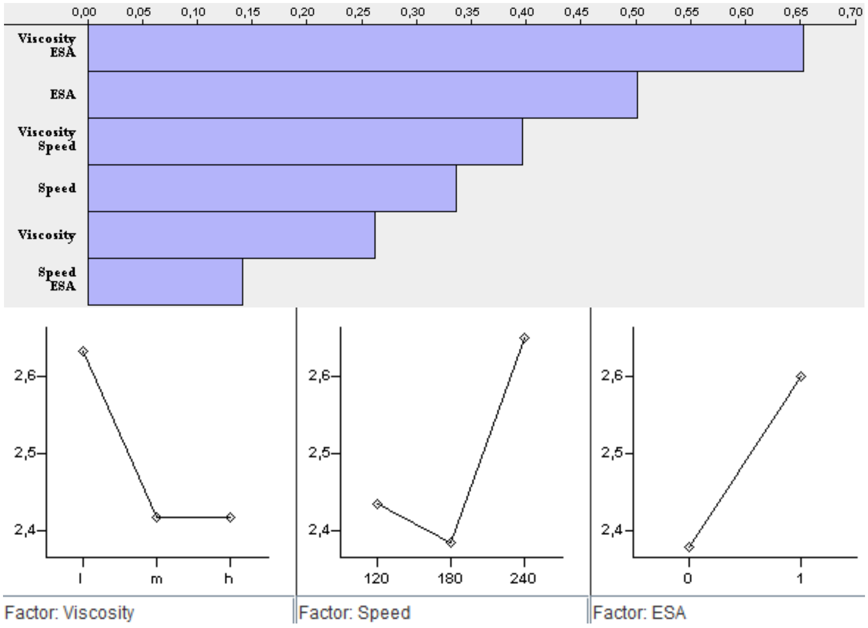

Figure 8: ANOVA evaluation of SCTV for 75 %
Pareto diagram (x-axis: ratio between critical value of f-distribution and factor's value) and mean values of the test points with respective factor level (y-axis: dSCTV value)

The statement from 4.1 that the viscosity has by far the highest influence, is reflected by this evaluation for 25 % and 50 %. It is indeed the only significant factor. ESA seems to be of slightly higher importance than speed, however both are not significant. The mean values show this finding directly. The slope between the averaged dSCTV values of the factor levels is maximal with viscosity. This is, however, different on paper substrates, where ESA plays a much more pronounced role due to the higher roughness of the paper compared to film.

The 75 % tone value offers a completely different picture. As in this range spreading no longer plays a role because no additional white areas can be covered, the effects are indeed all well below the significance threshold with an interaction of viscosity and ESA still as the strongest factor. Please note the much smaller spread of the mean values in the mean value diagram.

5. Conclusion and outlook

A model for the effect of different degrees of spreading of a dot was presented, based on the Murray-Davies formula and the Lambert-Beer absorption law, as well as on geometric considerations for spreading. With the help of this model, it can be shown that a more spreading dot with the same ink volume absorbs more and thus appears darker than a less spreading dot. The effect of different printing conditions, changed viscosity, strength of ESA and printing speed on dot gain i.e. SCTV were discussed. Ink viscosity was assumed to be the strongest factor, followed by ESA and printing speed. This could be quantified with the help of a design of experiment, where viscosity showed to be the only factor of major significance.

Further interesting dependencies could be demonstrated in the evaluation of the print test. However, the details of these are beyond the scope of this article.

Acknowledgements

We kindly thank Pauline Brumm, Thorsten Euler and Lara Philipp for their contribution in this elaborate print trial and their part of the sample and data preparation. We kindly thank Siegwerk for providing printing inks.

References

Backhaus, K., Erichson, B., Plinke, W. and Weiber, R., 2018. *Multivariate Analysemethoden: Eine anwendungsorientierte Einführung.* 16th ed. Berlin, Heidelberg: Springer.

Beilenhoff, S., 2011a. Troubleshooting im Verpackungstiefdruck. *Flexo+Tiefdruck*, 22(5), pp. 14–16.

Beilenhoff, S., 2011b. Troubleshooting im Verpackungstiefdruck. *Flexo+Tiefdruck,* 22(6), pp. 22–24.

Brumm, P., Lindner, N., Weber, T.E., Sauer, H.M. and Dörsam, E., 2021a. A deep learning approach for the classification task of gravure printed patterns. In: C. Ridgway, ed. *Advances in Printing and Media Technology: Proceedings of the 47th International Research Conference of iarigai.* Athens, Greece, 19–23 September 2021. Darmstadt: iarigai, pp. 2–9. https://doi.org/10.14622/Advances_47_2021.

Brumm, P., Weber, T.E., Sauer, H.M. and Dörsam, E., 2021b. Ink splitting in gravure printing: localization of the transition from dots to fingers. *Journal of Print and Media Technology Research*, 10(2), pp. 81–93. https://doi.org/10.14622/JPMTR-2016.

Brumm, P., Sprinzing, T., Euler, T., Galus, M., Weichmann, A. and Dörsam, E., 2022. *Creation of a comprehensive high-resolution image data set on an industrial web press to investigate hydrodynamic pattern formation in gravure printing.* In: C. Ridgway, ed. *Advances in Printing and Media Technology: Proceedings of the 48th International Research Conference of iarigai.* Greenville, USA, 19–21 September 2022. Darmstadt: iarigai, pp. 109–115. 10.14622/Advances_48_2022_08.

Deutsches Institut für Normung, 2019. *DIN EN ISO 2431 Paints and varnishes – Determination of flow time by use of flow cups (ISO 2431:2019, Corrected version 2019-09)*. Berlin: ISO.

Grau, G., Cen, J., Kang, H., Kitsomboonloha, R., Scheideler, W.J. and Subramanian, V., 2016. Gravure-printed electronics: recent progress in tooling development, understanding of printing physics, and realization of printed devices. *Flexible and Printed Electronics*, 1(2): 023002. https://doi.org/10.1088/2058-8585/1/2/023002.

Hübner, G., 1991. *Ein Beitrag zum Problem der Flüssigkeitsspaltung in der Drucktechnik.* Dissertation. Technische Hochschule Darmstadt. https://doi.org/10.25534/tuprints-00013550.

International Organization for Standardization, 2017. *ISO 20654:2017 Graphic technology – Measurement and calculation of spot colour tone value*. Geneva: ISO.

Joshi, A.V., 2016. Effect of electrostatic assist and gravure process parameters on voids and dot skips reduction in shrink PVC film. *Journal of Coatings Technology and Research*, 13(3), pp. 527–543. https://doi.org/10.1007/s11998-015-9774-0.

Kumar, S., 2015. Liquid transfer in printing processes: liquid bridges with moving contact lines. *Annual Review of Fluid Mechanics*, 47(1), pp. 67–94. https://doi.org/10.1146/annurev-fluid-010814-014620.

Kunz, W., 1975. Ink transfer in gravure process. In: *TAGA Proceedings 1975: Annual meeting of the Technical Association of the Graphic Arts*. Toronto, Ontario, 1975. Rochester, NY, USA: TAGA, pp. 151–176.

Montgomery, D.C., 2021. *Design and analysis of experiments.* 10th ed. Hoboken, NJ, USA: Wiley.

Weichmann, A., 2015. *GravureQ: commercially available software for mottle and missing dots analysis*. Hochschule der Medien Stuttgart, Germany.